Destruction of preferential accumulation using Lorentz force interactions.

KARNIK, A. and SHRIMPTON, J.

2008

DESTRUCTION OF PREFERENTIAL ACCUMULATION USING LORENTZ FORCE INTERACTIONS

Aditya Karnik*, John Shrimpton°

*Research Student, Energy Technology Research Group, School of Engineering Sciences, University of Southampton, Southampton. SO17 1BJ. UK. Email – aditya.karnik@soton.ac.uk
°Senior Lecturer, Energy Technology Research Group, School of Engineering Sciences, University of Southampton, Southampton. SO17 1BJ. UK. Email – john.shrimpton@soton.ac.uk

ABSTRACT
The effect of electric charge, residing on particles, upon the phenomenon of preferential accumulation is investigated using direct numerical simulations of forced isotropic turbulence. It is well known that particles with a certain range of Stokes numbers preferentially accumulate, or de-mix, due to action of turbulent motion. Here it is shown that charged particles interact with each other through an electric field generated by non-uniformity of particle distribution. This interaction mitigates preferential accumulation at a bulk charge density level that is practically relevant and commensurate with the first few centimetres of a spray plume, the region where non-homogeneous particle concentration typically forms. It is suggested that use of electric charge could be useful in improving mixture preparation for spray combustion applications.

1. INTRODUCTION

Understanding the interaction between particles and turbulence is a formidable task given the range of length and time scales present in a turbulent flow. One phenomenon which has been thoroughly researched is "preferential accumulation" or "de-mixing" of particles in certain Stokes number range. The review by Eaton and Fessler [1] demonstrates that preferential accumulation takes place in a range of flows including shear flows, wall-bounded flows and homogeneous turbulence. They also examined the mechanisms leading to this phenomenon and found that the same basic mechanisms are active in all these flows. The use of computational methods, such as point particle DNS, have proven to be a valuable tool for probing such phenomenon. In order to preserve accuracy, the flow configurations studied are generally limited to homogeneous isotropic turbulence, homogeneous shear flow, homogeneous plane strain, and homogeneous axi-symmetric expansion and contraction. The present study uses a point particle DNS code, PANDORA, to simulate mono-sized particles in homogeneous isotropic turbulence. Here we focus on use of electric charge, residing on particles, to mitigate preferential concentration.

Dilute turbulent particle flows are classified as one-way coupled or two-way coupled based on the coupling between the phases [2]. One-way coupled studies generally focus on particle dispersion issues while two-way coupled studies investigate modulation of turbulence due to inertial particles. In this work, we are interested in particle dispersion and thus all simulations reported in this study are one-way coupled. Also, the volume fraction of particles is in the dilute regime and thus particle-particle collisions are not considered.

Here we briefly review work on preferential concentration with a particular focus on DNS studies. One of the earliest observations of preferential accumulation was in a computational study by Squires and Eaton [3]. They found that particles tend to accumulate in regions of low vorticity and high strain. Interestingly they observed a non-monotonic dependence of the phenomenon on Stokes number.

Preferential accumulation was most pronounced for the intermediate Stokes number (0.15), based on integral scale, used in their simulations. The Taylor Reynolds number in their simulation was $Re_\lambda = 38.7$ and trajectories of 10^6 particles were followed. Wang and Maxey [4] performed DNS of heavy particles in homogeneous isotropic turbulence to investigate settling velocities of particles. They found that maximum settling velocity occurs when particle response time and drift velocity were of the order of Kolmogorov scales. They quantified the non-homogeneity in the particle distribution using a measure D_c, which is an indicator of deviation from uniform distribution. The results for 48^3 grid points ($Re_\lambda = 31$) clearly indicate maximum accumulation for Stokes number around 0.13. It should however be noted that the measure D_c is sensitive to the bin size used for binning the particles. Experimental work by Fessler et al. [5] investigated the dependence of preferential concentration on Stokes number at the centerline of a channel flow, which approximates homogeneous turbulence. They found that maximum deviation from randomness is observed for Stokes number, based on Kolmogorov scale, approximately one. They also found that the distance between particle clusters is much larger than scales at which preferential accumulation occurs. They defined a scalar parameter D to indicate deviation from randomness, which we have also used to quantify our results. The measure D basically quantifies deviation of particle concentration field from a random distribution. Hogan and Cuzzi [6] used D and D_c measures, among others, to quantify the preferential accumulation in their simulations. They found that the non-uniformity in particle distribution is most pronounced for Stokes number based on dissipation time scale equal to one.

While the effect of particle time constant (or Stokes number) has been systematically studied in literature, the effect of turbulence intensity has not been researched thoroughly. This is important if the findings established for low Reynolds numbers have to be extrapolated to real-world situations. Recently Scott et al. [7] showed that the turbulence intensity, characterized by the Taylor Reynolds number limits

the extent of preferential accumulation. This was shown using three measures of preferential accumulation - the D measure (as defined by Fessler et al. [5]), the D_c measure (as defined by Wang and Maxey [4]), and also the correlation between the particle number density and fluid enstrophy. This was also confirmed by extrapolating the trend to experimental measurements obtained by Fessler et al.[5] .

To summarise the introduction this far, the interaction of particles with fluid turbulence is a complex physical process, and the phenomenon of preferential accumulation is one result of this complexity. It has been well documented in terms of the particle Stokes number, in both one and two way coupled simulations, and also experimental work where homogeneous turbulence is reasonably approximated. Recently, the dependence of preferential concentration phenomenon on turbulence intensity has been quantified.

Eaton and Fessler [1] reflect upon number of practical applications where preferential accumulation might play a significant role. These applications range from coal fired combustors to electrostatic precipitators. For applications such as combustion, accumulation of particles in vortex structures is a problem because of non-uniform fuel vapor - air mixture preparation. This in turn leads to fuel rich and lean regions and combustion process will not be efficient and may produce unwanted emissions.

Typically, once the liquid primary atomization process has completed, the only means to modify the drop trajectory is via the fluid mean and fluctuating flow fields. Given the possibility of de-mixing of particle population due to interaction with dissipation scales of fluctuating velocity, this represents a problematic situation. This rules out using fluid velocity field to obtain uniform particle concentration. Given the above, what is ideally required is an intelligent body force which switches itself "on" once the particle distribution becomes non-uniform. Here we evaluate the viability of using Lorentz force to destroy the accumulation effect. The Lorentz force is the force exerted by an electric field at the particle location, with charge residing on that particle. In this work, we estimate the bulk charge density (amount of charge per unit volume of continuum) required to substantially reduce preferential accumulation.

Charging of droplets has already been proposed as a means to improve diluteness of sprays. Bellan [8] developed a model to demonstrate feasibility of charging fuel sprays in diesel engines. It was argued that a dilute spray would lead to lower soot formation and thus reduction in pollutant emissions. Charged injection atomizers are capable of generating electrically charged sprays of insulating hydrocarbon liquids and have been developed and refined. Electrically charged sprays offer several benefits like lack of droplet agglomeration and a control on the droplet size distribution and spray plume shape. Addition of electric charge leads to breakup of the jet by overcoming the balancing force due to surface tension. This leads to smaller mean diameters of the droplets and furthermore larger spray cone angles due to electrical repulsion between them. Details of spray characteristics of charge injection atomizers could be obtained from Rigit and Shrimpton [9].

The rest of the paper is organised as follows. Section 2 presents a case for using electric charge on particles and the need of a detailed study thereof. Section 3 presents details of the pseudo-spectral method, code organization, initialization and forcing method. In section 4 results from a comprehensive set of mono-sized simulations are presented and discussed. Section 5 lists the conclusions from this study.

2. MOTIVATION FOR DETAILED STUDY OF CHARGED PARTICLE SIMULATIONS

The degree of reduction of preferential accumulation for a given Stokes number, turbulence intensity and bulk charge density is by no means obvious. For a uniform distribution of particles in the domain, the electric field generated will be null. In such a state, interaction with underlying turbulence will centrifuge the particles away from vortex cores with which they interact and lead to preferential concentration. This non-uniformity would produce a net electric field, the strength of which will be governed by the bulk charge density levels. For adequate levels of bulk charge density, the Lorentz force on a particle would be of sufficient magnitude to overcome turbulent interactions. In such cases, non-uniformity of particle distribution would be reduced accompanied by commensurate weakening of the Lorentz force. This points to a possibility of periodicity in "activity" of Lorentz force. On the other hand, simulations of "uncharged" particles [7] have demonstrated that preferential concentration attains a stationary state consistent with the stationarity of fluid statistics.

The above discussion lends itself to the following questions – "Would charged particle simulations lead to a stationary particle concentration field?". And if so, "How would the stationary magnitude of preferential concentration compare with the "uncharged" case?". The attempt to answer these questions is the underlying motivation for this particular study.

3. OVERVIEW OF SIMULATIONS

The computational method used for this study is point-particle DNS. PANDORA, a point-particle DNS code, has been used to obtain the results presented in this study. Here we describe a few basic features of this code. For more details about the code, the reader is referred to Scott [10].

3.1 Fluid Turbulence

PANDORA employs the pseudo-spectral method for simulating homogeneous isotropic turbulence. This method was originally developed for homogeneous isotropic turbulence by Orszag and Patterson [11] and later extended to more interesting flows by Rogallo [12].

The code is based on the incompressible Navier-Stokes equations in the physical rotational form

$$\frac{\partial \overline{u}_f}{\partial t} + \left(\overline{\omega}_f \times \overline{u}_f \right) = -\frac{1}{\rho_f} \nabla P_m + \nu_f \nabla^2 \overline{u}_f \qquad (1)$$

where P_m is the modified pressure term,

$$P_m = P + \frac{1}{2} \rho_f \left| \overline{u}_f \right|^2 \qquad (2)$$

This form of the Navier-Stokes equations semi-conserves kinetic energy and has been shown to be the most stable form for numerical simulations [13].

In a Fourier-spectral formulation, the velocity field is decomposed into orthogonal Fourier modes. It is

straightforward to show that the incompressible Navier-Stokes equations can now be represented in Fourier space by equations 3 and 4.

$$\overline{\kappa} \cdot \overline{u}_f(\overline{\kappa}) = 0 \qquad (3)$$

$$\frac{\partial \overline{u}_f(\overline{\kappa})}{\partial t} = -\nu_f \kappa^2 \overline{u}_f(\overline{\kappa}) - \left(\overline{\omega}_f(\overline{\kappa}) \times \overline{u}_f(\overline{\kappa})\right) \qquad (4)$$
$$+ \frac{\overline{\kappa}}{\kappa^2}\left[\overline{\kappa} \cdot \left(\overline{\omega}_f(\overline{\kappa}) \times \overline{u}_f(\overline{\kappa})\right)\right]$$

Evaluation of the non-linear term, $\left(\overline{\omega}_f(\overline{\kappa}) \times \overline{u}_f(\overline{\kappa})\right)$ in the spectral domain proves extremely expensive and the velocity information is transformed from Fourier space to real space, the non-linear term is evaluated, and transformed back to Fourier space. Evaluation of the non-linear terms introduces aliasing errors and in the PANDORA code the errors are eliminated using a simple truncation method. The PANDORA code simulates isotropic turbulence in a cubical triply periodic domain of volume L^3. In all simulations the domain is of size $L = 2\pi$ which has the advantage of integer wave-numbers in Fourier space. This real space domain corresponds to a Fourier space domain of size N^3 Fourier modes. However, conjugate symmetry of the complex Fourier modes means that only $N^2(N/2 + 1)$ nodes require storage.

Initialization and forcing. The velocity field is initialized using the (corrected) method described in Rogallo [12] to conform to a pre-specified energy spectrum and to satisfy continuity. Both the fluid and particle fields are advanced using the third order Runge-Kutta scheme of Williamson [14]. The time step is calculated according to a predefined Courant Fredricks Levy (CFL) number. All simulations in this study use the CFL number CFL = 0.75 and the time step Δt is adjusted dynamically during the simulation.

In order to obtain a statistically stationary simulation without decay of the energy spectrum, it is necessary to input energy by forcing the large scale motions of the flow. The forcing scheme used in the PANDORA code is an Uhlenbeck-Ornstein stochastic process, as defined by Eswaran and Pope [15]. Forcing of the large scales is achieved by the addition of a forcing acceleration to the Navier-Stokes equation in wave space form within a sphere of radius $K_F = 2\sqrt{2}\kappa_0$. The forcing scheme is characterised by the following non-dimensional quantities

$$\varepsilon^* = \sigma_F^2 T_L : \text{Re}^* = \varepsilon^* \kappa_0^{-4/3}/\nu_f : T_L^* = T_L \varepsilon^{*1/3} \kappa_0^{2/3} : \kappa_{max}/\kappa_0 : K_F/\kappa_0 \quad (5)$$

where Re* is the forcing Reynolds number, ε* is the forcing dissipation and T_L* is the non-dimensional forcing time scale.

Simulation parameters. The fluid turbulence intensity is characterized by the Taylor Reynolds number. In this work, three Taylor Reynolds numbers have been reported - 24.15,

Parameter / Variable	Tabulated	V32	V64	V128
N - grid size	N	32	64	128
ν_f - kinematic viscosity	ν_f	0.025	0.025	0.025
K_F - largest forced wave number	K_F/κ_0	$2\sqrt{2}$	$2\sqrt{2}$	$2\sqrt{2}$
κ_{max} - largest resolved wavenumber	$\kappa_{max}\langle\eta\rangle$	1.306	1.269	1.32
κ_0 - smallest resolved wavenumber	$\kappa_0\langle\eta\rangle$	0.0754	0.035	0.018
$l = \frac{1}{3}L_{i,i}$ - integral length scale	$k_0\langle l\rangle$	1.22	1.00	0.85
L_ϵ - turbulent length scale	$\langle L_\epsilon/l\rangle$	0.961	1.61	2.05
λ - Taylor microscale	$\langle\lambda/l\rangle$	0.598	0.49	0.38
η - Kolmogorov length scale	$\langle\eta/l\rangle$	0.062	0.035	0.021
T_E - eddy turnover time	$\langle l/u'\rangle$	1.477	0.389	0.135
τ_η - Kolmogorov time scale	$\langle\tau_\eta\rangle/T_E$	0.228	0.049	0.013
k - turbulent kinetic energy	$\langle k\rangle$	1.036	9.947	59.72
$u' = (2k/3)^{1/2}$ - turbulence intensity	$\langle u'\rangle$	0.829	2.57	6.31
ϵ - dissipation	$\langle\epsilon\rangle$	0.490	10.64	145.1
$\text{Re}_l = u'l/\nu_f$ - Reynolds number	$\langle\text{Re}_l\rangle$	40.50	102.8	214.4
$\text{Re}_\lambda = u'\lambda/\nu_f$ - Taylor Reynolds number	$\langle\text{Re}_\lambda\rangle$	24.15	49.85	81.10

Table 1. Run parameters and averaged variables calculated from PANDORA code validation runs for 32^3, 64^3, 128^3 domains. Angled brackets $\langle\rangle$ denote the time averaged stationary value.

49.85, 81.1 corresponding to 32^3, 64^3 and 128^3 grid configurations respectively. Details of the fluid turbulence are given in Table 1.

3.2 Particle implementation

The particles are distributed across all processes and each particle resides on the process containing the appropriate section of the real space domain and velocity field. The particle trajectories are calculated using the real space velocity field, and advanced in time using the same third order Runge-Kutta scheme as used for the fluid phase. The position of a particle is calculated according to the following ordinary differential equation

$$\frac{d\overline{X}}{dt} = \overline{U} \qquad (6)$$

$$\frac{d\overline{U}}{dt} = -\frac{1}{\tau_u f_u}\left(\overline{U} - \overline{u}^*\right) + \frac{q}{m}\overline{E}^* \qquad (7)$$

Where $\overline{u}^*$ is the fluid velocity at particle location and $\overline{E}^*$ is the electric field at particle location. The fluid velocity and electric field are interpolated to particle location using a third-order polynomial method. The particle drag function f_u and particle Reynolds number Re_p are calculated as follows [16],

$$f_U = 1 + 0.15\,\text{Re}_p^{0.687} \qquad (8)$$

$$\text{Re}_p = \frac{\left|\overline{U} - \overline{u}^*\right|\phi}{\nu_f} \leq 800 \qquad (9)$$

Where, ϕ is the particle diameter and ν_f is fluid kinematic viscosity. The particle relaxation time (or time constant) can be calculated as

$$\tau_U = \frac{18 \rho_f \nu_f}{\rho \phi^2} \tag{10}$$

The electric field over the domain is given by the divergence theorem

$$\nabla \cdot \overline{E} = \frac{nq}{\varepsilon_0} \tag{11}$$

Where, n is the particle number density (number of particles per unit volume), q is th charge on a single particle, ε_0 is the permittivity of free space (8.854×10^{-12} F/m)

PANDORA, being a pseudo-spectral code, it is convenient to evolve the electric field in spectral space. Using a Fourier series representation, the electric field is expressed as a truncated Fourier series

$$\overline{E}(\overline{x}) = \sum_\kappa \overline{E}(\overline{\kappa}) e^{i \overline{\kappa} \cdot \overline{x}} \tag{12}$$

The Fourier space equivalent of equation 12 is then given by

$$\overline{\kappa} \cdot \overline{E}(\overline{\kappa}) = \overline{S}(\overline{\kappa}) \tag{13}$$

where, $\overline{S}(\overline{\kappa})$ is the Fourier mode (at wave-number $\overline{\kappa}$) of the source term nq/ε_0. The real-space electric field is obtained by Fourier transform (Eqn. 12).

FFTW library is used to transform the electric field from Fourier-space to real-space.

The particles in these simulations are stochastic as far as attaining the required charge density levels are concerned. It implies that a single computational particle represents charges present on an ensemble of particles. The charge placed on a single real particle is limited by the Rayleigh limit. The Rayleigh limit (Eqn. 14) represents the maximum charge that can be placed on a liquid droplet.

$$Q_{ray} = 8\pi \sqrt{\gamma \varepsilon_0 r_d^3} \tag{14}$$

where, γ is the surface tension coefficient and r_d is the radius of the droplet. The Rayleigh number is the actual charge present on a droplet as a fraction of the Rayleigh limit. For all simulations in this study, surface tension coefficient of $\gamma = 0.05$ N/m and Rayleigh number of *0.8* were used.

3.3 Averaging and statistics

All statistics have been obtained from identical realisations of the turbulent carrier flow. Identical realisations were achieved by starting all simulations using restart files generated at end of the validation runs and using

	V32	V64	V128
C - CFL Number	0.75	0.75	0.75
K_F - largest forced wave number	$2\sqrt{2}$	$2\sqrt{2}$	$2\sqrt{2}$
N_F - number of forced wave modes	92	92	92
ϵ^* - dimensionless forcing dissipation rate	0.001	0.014	0.276
T_L^* - dimensionless forcing time scale	0.100	0.078	0.044
Re^* - dimensionless forcing Reynolds number	4.310	9.730	26.043

Table 2. Time step and forcing parameters for 32^3, 64^3, 128^3 validation runs.

the forcing parameters detailed in Table 2. Particles were initialised at random positions within the computational domain and released with initial velocity equal to the local fluid velocity. To ensure identical realisations, the random number generator in PANDORA was seeded with the same number prior to particle initialisation, and reseeded prior to advancement of the fluid field. This guaranteed that the particles were initialised in the same positions for each realisation (assuming equal number of particles) and also ensured that the fluid realisation was identical each time, independent of the number of particles used since the flow is one way coupled.

Both Eulerian and Lagrangian statistics were collected at every time step during the simulation. Lagrangian statistics were ensemble averaged across all particles. The Eulerian statistics were volume-averaged for all nodes in the computational domain. All statistics were written to file at each time step and subsequently time averaged at the end of the simulation. An initial period at the start of the simulation was disregarded when time averaging to allow the particles to obtain statistically stationary state within the flow. The particle number density field was calculated simply by counting the number of particles in each volume surrounding a computation node and dividing by the total number of particles.

The code used for these simulations has been extensively tested and validated against experimental data for freely decaying isotropic turbulence and other simulations of forced statistically stationary isotropic turbulence. Brief details may be found in Scott et al. [7] and full details may be obtained from Scott [10].

4. RESULTS AND DISCUSSION

The work presented here can be viewed as an extension of the findings discussed in Scott et al. [7] and the reader is encouraged to first review these findings. In this section, we report results obtained from a set of monosized simulations for a range of values of following parameters - Taylor Reynolds numbers, Stokes numbers and bulk charge density levels. The effect of each of these parameters is systematically studied. The Taylor Reynolds numbers reported in this work are – 24.2, 49.9, 81.1. The Stokes numbers reported are 0.25, 1.00, 2.00 and 4.00, where the Stokes number is based on the integral time scale of the fluid. The bulk charge density levels simulated for each combination of Reynolds number and Stokes number are 5, 10, 25, 50 and 100 μC/m³. Preferential accumulation has been quantified using three measures - D_c as defined by Wang and Maxey [4], D defined by Fessler et al. [5],
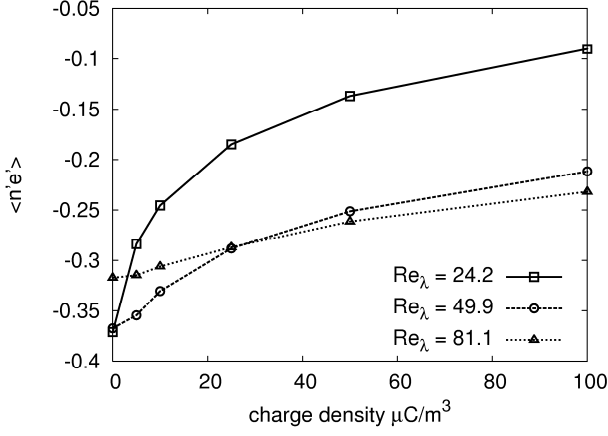
Fig. 1. Variation of $\langle n'e' \rangle$ with bulk charge density for $\text{Re}_\lambda = 24.2, 49.9, 81.1$.
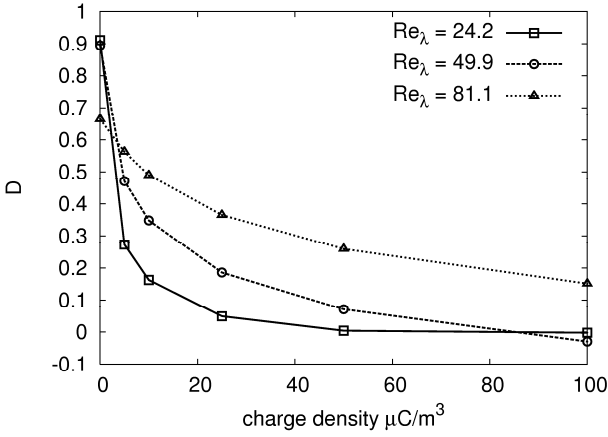

Fig. 2. Variation of D with bulk charge density for $\text{Re}_\lambda = 24.2, 49.9, 81.1$.
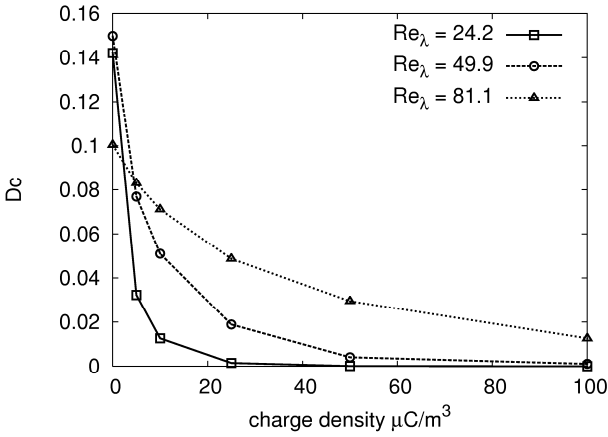

Fig. 3. Variation of D_c with bulk space charge density for $\text{Re}_\lambda = 24.2, 49.9, 81.1$.

Fig. 4. Variation of $\langle n'e' \rangle$ with Stokes number for different charge density levels at $\text{Re}_\lambda = 24.2$.

Fig. 5. Variation of $\langle n'e' \rangle$ with Stokes number for different charge density levels at $\text{Re}_\lambda = 49.9$.

Fig. 6. Variation of $\langle n'e' \rangle$ with Stokes number for different charge density levels at $\text{Re}_\lambda = 81.1$.

and a Eulerian correlation between particle number density and fluid enstrophy [10].

Initially we look at results for a constant Stokes number to single out the effect of space charge density. Figures 1, 2 and 3 show the effect of putting increasing charge density on each of the accumulation sensors - $\langle n'e' \rangle$, D and D_c. Clearly putting more charge in the domain leads to significant
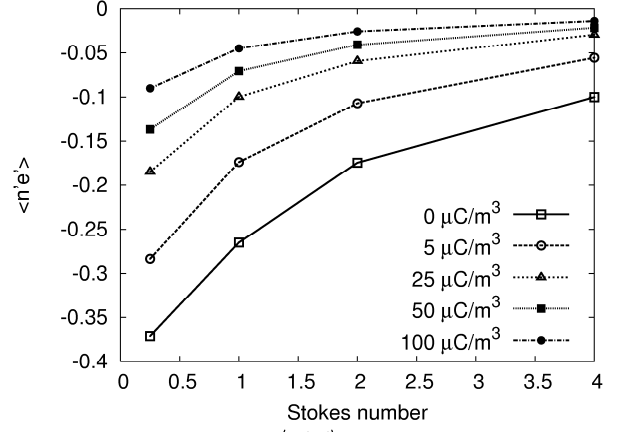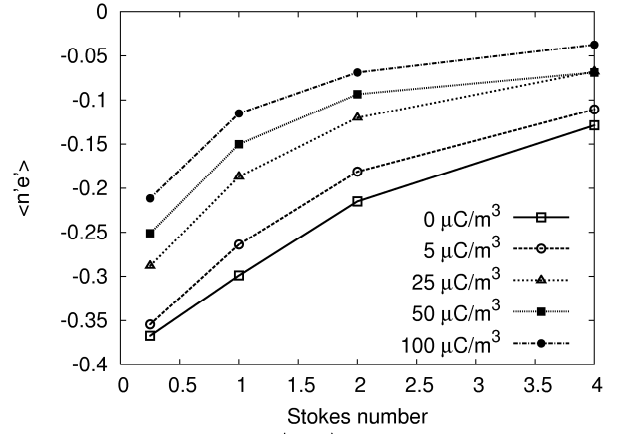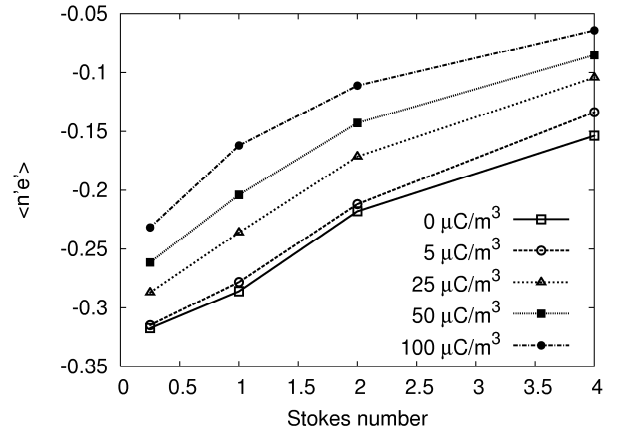
reduction in preferential accumulation. Space charge density of 50 μC/m^3 is sufficient to substantially eliminate the non-uniformity in particle distribution. While the sensors D and D_c look purely at the particle distribution, the sensor $\langle n'e' \rangle$ tracks the tendency of particles to accumulate in low-vorticity areas. Reduction of $\langle n'e' \rangle$ with increasing space charge
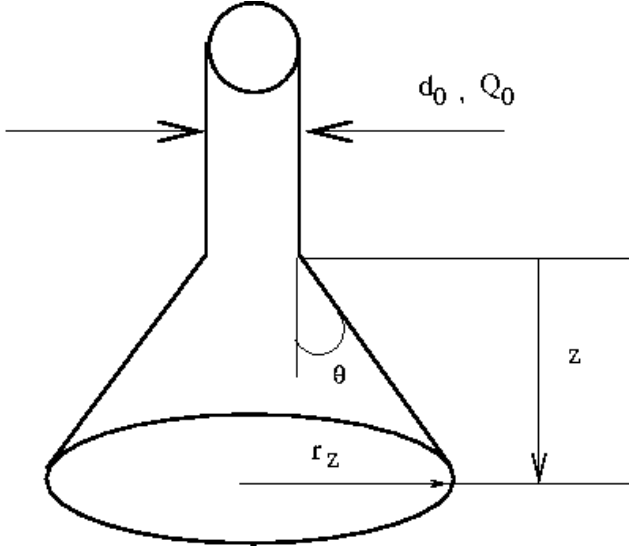
Fig. 7. Schematic of a spray released from a charged injection atomizer.

density points to more particles being able to sustain themselves in high-vorticity regions. This indicates that the Lorentz force enables the particles to mitigate the centrifugal effects in the core of vortices. For zero charge on particles, in the regime of Stokes numbers used in present work, the accumulation phenomenon monotonically reduces with an increase in Stokes number. It is not immediately obvious if this trend would sustain itself in presence of Lorentz forces. Figures 4, 5 and 6 show that the Stokes number dependence is retained in presence of charges.

Turbulence intensity has been shown to limit the extent of preferential accumulation by Scott et al. [7]. However the role played by turbulence intensity in presence of inter-particle Lorentz forces is modified. Figures 1, 2 and 3 indicate that while at lower Reynolds number, the effect of putting charge produces dramatic reduction in accumulation, the effect at higher Reynolds numbers is slightly damped. This could be explained by the more energetic structures at higher Reynolds number requiring greater force to overcome their influence. This points to possibility of requiring greater space charge levels at higher Reynolds numbers.

Here, we work out the bulk charge density levels prevalent in practical charged injection atomizers. Figure 7 shows a schematic of a spray from a charged injection atomizer. We assume that the liquid jet is initially a cylinder of diameter d_0 and volume charge density, Q_0 (there is no gas in the mixture). The spray plume then expands as a cone, entraining air and reducing the bulk charge. For a spray half-angle of θ, the spray radius at any section z, is given by,

$$r_z = \frac{d_0}{2} + z \tan \theta \qquad (15)$$

Assuming velocity of the plume does not change, then the volume charge density is a function of the cross-sectional area. The volume charge density at any section z is then given by Eqn. 16.

$$Q_z = \frac{Q_0}{1 + \dfrac{4z \tan \theta}{d_0} + \dfrac{4z^2 \tan^2 \theta}{d_0^2}} \qquad (16)$$

For a spray with initial diameter, $d_0 = 500 \mu m$, initial charge density, $Q_0 = 0.5$ C/m^3 and spray angle of 45°, the charge level found in this study (50 μC/m^3) corresponds to an area about 2 cm from the nozzle tip.

The assumption of constant velocity is rather poor, whereas in reality the spray plume will decelerate and the downstream particle concentration would increase. Therefore the estimates given here of bulk specific charge (spray + air) can be considered conservative.

It is seen that the levels of charge required to significantly reduce the preferential accumulation are within that capable of charged injection atomization devices currently available.

5. CONCLUSIONS

Forced isotropic simulations of dispersed phase flows have been performed using a well validated code. It has been observed that it is possible to mitigate the phenomenon of preferential accumulation using charges residing on particles. For this purpose, charges have been placed on a mono-sized particle population and the resulting accumulation of particles has been quantified using well-known measures.

The main findings in this investigation are summarised as follows:

- Bulk charge density level of 50 μC/m^3 is sufficient to significantly destroy preferential accumulation. This has been consistently observed using different sensors for preferential concentration.
- Charged particle systems continue to exhibit same trends with Reynolds and Stokes numbers as the charge-free cases.
- The required charge density level mentioned above is attainable within 2cms from tip of a nozzle in practical charge injection atomizers.

In practical atomizers, the first non-homogeneous clustering of particles tends to occur in the first few centimeters from the nozzle. Thus placing charges on particles holds the promise of creating a homogeneous mixture downstream of the spray. This is especially useful in the context of combustion where de-mixing of the fuel-vapour mixture results in incomplete combustion and formation of soot and other pollutants.

NOMENCLATURE

Symbol	Quantity	SI Unit
t	Time	s
q	Electric charge	C
n	Particle number density	m^{-3}
m	Particle mass	Kg
ρ	Particle density	Kg m^{-3}
κ	Wavenumber	m^{-1}
ε_0	Permittivity of free space	F m^{-1}
ϕ	Particle diameter	M
γ	Surface tension coefficient	N m^{-1}
$\overline{u}_f$	Fluid velocity	m s^{-1}
$\overline{\omega}_f$	Fluid vorticity	Rad s^{-1}

NOMENCLATURE

ρ_f	Fluid density	Kg m^{-3}
ν_f	Fluid viscosity	m^2 s^{-1}
P_m	Modified pressure	N m^{-2}
Re_p	Particle Reynolds number	Dimensionless
$\overline{u}_f(\overline{\kappa})$	Fourier component of fluid velocity	m s^{-1}
κ_F	Maximum wavenumber of forced modes	m^{-1}
κ_0	Minimum wavenumber	m^{-1}
Re^*	Forcing Reynolds number	Dimensionless
T_L^*	Non-dimensional forcing time-scale	Dimensionless
ε^*	Forcing dissipation	m^2 s^{-3}
$\overline{X}$	Particle position vector	m
$\overline{U}$	Particle velocity vector	m s^{-1}
τ_U	Particle relaxation time	s
f_U	Particle drag function	Dimensionless
r_d	Droplet radius	m

REFERENCES

[1] J.K. Eaton and J.R. Fessler, Preferential Concentration of Particles by Turbulence, Int. J. Multiphase Flow, Vol. 20, pp. 169-209, 1994.

[2] C.T. Crowe, T.R. Troutt and J.N. Chung, Numerical Models for Two-Phase Turbulent Flows, Annu. Rev. Fluid Mech., Vol. 28, pp. 11-43, 1996.

[3] K.D. Squires and J.K. Eaton, Preferential Concentration of Particles by Turbulence, Phys. Fluids A, Vol. 3(5), pp. 1169-1179, 1991.

[4] L.P. Wang and M.R. Maxey, Settling Velocity and Concentration Distribution of Heavy-Particles in Homogeneous Isotropic Turbulence, J. Fluid Mech., Vol. 256 pp. 27-68, 1993.

[5] J.R. Fessler, J.D. Kulick and J.K. Eaton, Preferential Concentration of Heavy-Particles in a Turbulent Channel Flow, Phys. Fluids, Vol. 6(11), pp. 3742-3749, 1994.

[6] R.C. Hogan and J.N. Cuzzi, Stokes and Reynolds Number Dependence of Preferential Particle Concentration in Simulated Three-dimensional Turbulence, Phys. Fluids, Vol. 13(10), pp. 2938-2945, 2001.

[7] S.J. Scott, A.U. Karnik and J.S. Shrimpton, A Turbulence Limit for Preferential Accumulation, Submitted to Int. J. Heat Mass Transfer, 2008.

[8] J. Bellan, A New Approach to Soot Control in Diesel-Engines by Fuel-Drop Charging, Combustion and Flame, Vol. 51(1), pp. 117-119, 1983.

[9] A.R.H. Rigit and J.S. Shrimpton, Spray Characteristics of Charge Injection Electrostatic atomizers with Small-orifice Diameters, Atomization and Sprays, Vol. 16, pp. 421-442, 2006.

[10] S. Scott, PDF Based Method for Modelling Polysized Particle Laden Turbulent Flows without size class discretization, Ph.D. thesis, Imperial College London, 2006.

[11] S.A. Orszag and G.S. Patterson, Numerical Simulation of 3-Dimensional Homogeneous Isotropic Turbulence, Phys. Rev. Lett., Vol. 28(2), pp. 76-79, 1972.

[12] R. Rogallo, Numerical Experiments in Homogeneous Turbulence, NASA Tech. Memo. 81315, 1981.

[13] C. Canuto, M.Y. Hussaini, A. Quarteroni and T.A. Zang, Spectral Methods in Fluid Dynamics, Springer-Verlag, 1988.

[14] J.H. Williamson, Low-Storage Runge-Kutta Schemes, J. Comput. Phys., Vol. 35(1), pp. 48-56, 1980.

[15] V. Eswaran and S.B. Pope, An Examination of Forcing in Direct Numerical Simulations of Turbulence, Computers and Fluids, Vol. 16(3), pp. 257-278, 1988.

[16] R. Clift and J.R. Grace, Bubbles, Drops and particles, New York: Academic Press, 1978.